Meteorology and Atmospheric Physics (2021) 133:1355–1365
https://doi.org/10.1007/s00703-021-00814-0

ORIGINAL PAPER

Causes of the extreme drought event in Liaoning Province, China in July–August 2014

Min Jiao[1,2] · Wei Huang[3] · Liqiang Chen[1,2] · Fenghua Sun[1,2] · Zenghua Yu[2,4]

Received: 7 July 2020 / Accepted: 10 June 2021 / Published online: 25 June 2021

Abstract
Liaoning Province in China experienced an extremely severe drought event in July–August (midsummer) 2014. We investigated the features and related circulation anomalies of this drought event using observational data, NCEP/NCAR reanalysis datasets, and the NOAA extended reconstructed sea surface temperature dataset. Precipitation in Liaoning Province was very low in midsummer 2014, leading to the worst drought in the past 50 years. Water vapor diverged from Liaoning Province with a strong descending flow. Two factors facilitated this extreme drought event. The first was the teleconnections at mid- and high latitudes related to the East Asian–Pacific (EAP), Eurasian (EU), and Silk Road (SR) patterns. Rossby wave energy dispersed eastward along the EU pattern at high latitudes and along the SR pattern at mid-latitudes, reinforcing the centers of the geopotential height anomalies of the negative phase of EAP pattern. This resulted in the southward positioning of the western Pacific subtropical high (WPSH) and the weaker East Asian summer monsoon (EASM), leading to the drought event in Liaoning Province. The second factor affecting the drought event was anomalous thermal forcing over the northwestern Pacific, the Maritime Continental (MC) region, and the Indian Ocean. The sea surface temperature anomalies (SSTAs) were positive in the equatorial Pacific and most of the Indian Ocean and presented a positive–negative–positive sandwich structure from the warm pool of the western Pacific at low latitudes to high latitudes to the north of the equatorial Pacific and to the west of 160 °W. Anomalous winds converged over the Indo-China Peninsula and the MC region from the southern equatorial Indian Ocean and the western Pacific in the lower troposphere and converged into the Bay of Bengal and the western Pacific from the Japanese archipelago and east of the Indonesian islands in the upper troposphere, building an anomalous descending flow over Liaoning Province.

1 Introduction

There have been frequent drought events in China and Eurasia in recent years (Kim et al. 2011; Zhang et al. 2013, 2015; Schubert et al. 2014; Zhang and Zhou 2015; Barriopedro et al. 2012; Ma et al. 2019; Jiao et al. 2019). In July–August (midsummer) 2014, a severe drought event occurred in Liaoning Province. The lack of precipitation not only caused river levels in Liaoning Province to be unusually low and even dry up, but also had a serious impact on agricultural production and daily life, leading to large losses in the national economy (Jiao et al. 2018).

Liaoning Province is located in the south of northeast China on the east coast of the Eurasian continent, and therefore, has an East Asian monsoon climate. Precipitation is mainly concentrated in the summer months. Summer precipitation in Liaoning Province has significant interannual and interdecadal variations (Yang and Wang 2006; Li et al. 2014), but the long-term variation trend is unclear (Jiao et al. 2018; Li et al. 2014). The summer precipitation in this province is mainly affected by the East Asian summer monsoon (EASM) (Yang and Wang 2006). Large-scale circulation features influencing precipitation in Liaoning Province include the subtropical upper westerly jet, the western Pacific subtropical high (WPSH), the low-level jet, the westerly trough,

Responsible Editor: Stephanie Fiedler.

✉ Min Jiao
jiaomin@iaesy.cn

1 Institute of Atmospheric Environment, China Meteorological Administration, Shenyang 110166, China

2 Key Opening Laboratory for Northeast China Cold Vortex Research, Shenyang 110166, China

3 College of William and Mary, Virginia Institute of Marine Science, Gloucester Point, VA 23062, USA

4 Meteorological Disaster Monitoring and Warning Center of Liaoning Province, Shenyang 110166, China

the polar vortex, and the South Asian high (Jiao et al. 2018; Yang and Wang 2006; Li et al. 2014).

The Silk Road (SR, Lu et al. 2002; Enomoto et al. 2003) pattern propagating zonally in the subtropical westerly jet zone and the East Asian–Pacific (EAP, Huang and Li 1987) pattern propagating along the meridional direction on the coast of East Asia are the two most important teleconnection patterns affecting the East Asian summer climate anomalies (Huang et al. 2016). The continuous hot and dry summer of 2013 in the mid- and lower reaches of the Yangtze River (Wang et al. 2017) and the severe drought in northeast Asia during the summer of 2014 (Wang and He 2015) are all closely related to these teleconnection patterns. The summer droughts that occurred in north China in 1999 and 2000 were related to the Eurasian (EU, Wallace and Gutzler 1981) pattern (Wei et al. 2004). The dispersion of Rossby wave energy in the mid- and upper troposphere in the northern hemisphere plays an important part in the formation and maintenance of important circulation systems affecting the summer climate in China and the occurrence of extreme weather events (Wang et al. 2017; Wang and He 2015; Shi et al. 2009; Ke and Guan 2014; Xu et al. 2017; Li et al. 2016; Ye et al. 2019; Sun et al. 2019).

Sea surface temperature anomalies (SSTAs) have an important effect on anomalous summer precipitation in northeast China. The severe hot drought event that occurred in northeast China, the Korean Peninsula, and Japan during summer 2014 was related to the northeastern propagation of Rossby waves triggered by the Indian Ocean Dipole (Saji et al. 1999; Guan and Yamagata 2003). Analysis shows that SSTAs in the subtropical southeastern Pacific in the previous winter can trigger an alternating cyclone–anticyclone wave train spanning the northern and southern hemispheres from the key sea area to the northeast and cause an anomaly in the atmospheric circulation in mid- and high latitudes of the northern hemisphere, affecting summer precipitation in northeast China (Gao and Gao 2015). Analysis revealed that the decadal relationship between the Kuroshio sea surface temperature (SST) in winter and summer precipitation in northeast China changed from a weak positive correlation in 1950s to a strong negative correlation in recent years. In years with abnormal summer precipitation in northeast China, the thermal anomalies of the Kuroshio SST can cause an anomaly in the WPSH and intensify the cold vortex in northeast China, leading to the summer precipitation anomalies over northeast China (Gao and Gao 2014). Wang et al. (2016) found that the difference in the anomalous Kuroshio SST and its area of extension between two El Niño events could cause the deviation of the anomalous circulation along the East Asian coast, leading to the anomalous summer precipitation in northeast China in 1998 and 2010. The anomalous ocean heat content can also lead to blocking of the WPSH and the Okhotsk Sea high-pressure anomalies and, in turn, to the summer precipitation anomalies in northeast China (Wang et al. 2013). Studies have shown that the SSTAs in the warm pool region of the western Pacific Ocean can excite the planetary wave propagating to the northeast, thus forming the EAP/PJ (Pacific–Japan) pattern teleconnection (Wang and He 2015; Nitta 1987; Kurihara and Tsuyuki 1987). The SSTAs in the warm pool area of the western Pacific Ocean was a significant positive anomaly in summer 2014 and the SST in the northern Pacific Ocean was the warmest in the past 60 years. A strong pressure–temperature pattern was generated under the combined effect of these factors, which moved the WPSH anomaly southward and resulted in an unusually strong East Asian trough, leading to the anomalous southward location of the rain belt and an anomalous drought in northeast Asia (Wang and He 2015).

Although the cause of the severe summer drought in northeast Asia in 2014 has been analyzed, analysis specific to Liaoning Province, which was seriously affected by this event, is limited. The causes of summer precipitation anomalies in Liaoning Province analyzed from the perspective of the dispersion of Rossby wave energy, atmospheric teleconnections, and thermal forcing in mid- and high latitudes are also rare. We, therefore, studied the possible mechanism of formation of the extreme drought event in Liaoning Province during midsummer 2014 from the perspective of meteorological drought based on precipitation data from observational and reanalysis datasets.

2 Data and methodology

The data used in this study include the monthly National Centers for Environmental Prediction/National Center for Atmospheric Research (NCEP/NCAR) reanalysis datasets for midsummer during the time period 1981–2014 with 17 levels in the vertical direction and a grid mesh of $2.5° \times 2.5°$ (Kalnay et al. 1996), the monthly National Oceanic and Atmospheric Administration (NOAA) Extended Reconstructed Sea Surface Temperature (ERSSTv4) dataset with a grid mesh of $2° \times 2°$ for midsummer during the time period 1981–2014 (Smith et al. 2008), and daily precipitation data from 53 meteorological stations in Liaoning Province (Fig. 1a) during the time period 1962–2014. In this work, midsummer refers to the months of July and August. The climatological mean refers to the average values for the time period 1981–2010. Anomalies represent the deviation from the climatological mean.

The horizontal component of the wave activity flux (Takaya and Nakamura 1997, 2001) (the T-N flux) is used to diagnose the disturbance in the propagation of energy in the quasi-stationary planetary wave. The T-N flux is independent of the wave phase under the WKB approximation and is consistent with the local group velocity direction of

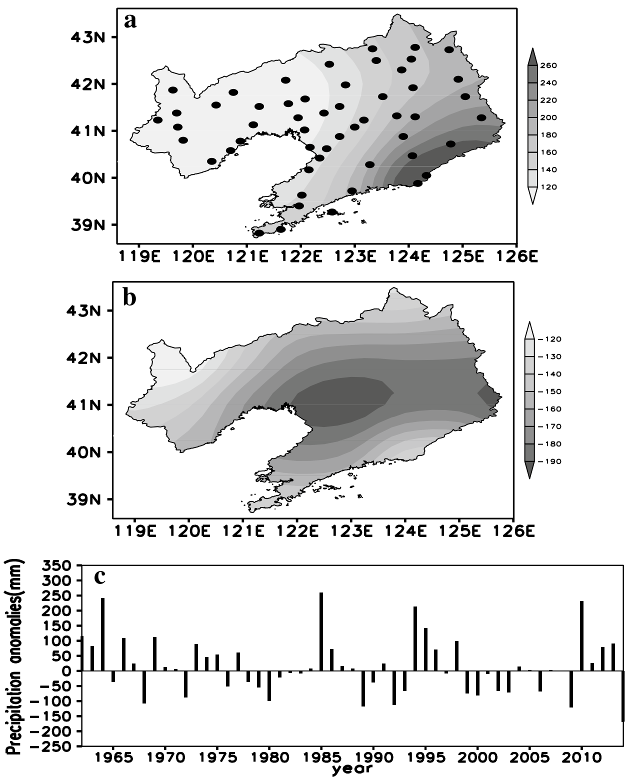

Fig. 1 **a** Locations of 53 stations in Liaoning Province (dots) and the distribution of total precipitation (shading; units: mm) during midsummer 2014. **b** Precipitation anomalies (mm) and **c** time series of precipitation anomalies (mm) averaged over Liaoning Province during midsummer in the time period 1962–2014

the stationary Rossby wave. The remainder of the T-N flux relative to the phase velocity is W_r, which is expressed on the pressure coordinate as

$$W_r = \frac{p}{2|U|}\begin{pmatrix} U(\psi'^2_x - \psi'\psi'_{xx}) + V(\psi'_x\psi'_y - \psi'\psi'_{xy}) \\ U(\psi'_x\psi'_y - \psi'\psi'_{xy}) + V(\psi'^2_y - \psi'\psi'_{yy}) \end{pmatrix},$$

where p is the pressure,U is the background flow ($U = U\, i + V\, j$), and ψ' is the quasi-geostrophic perturbation stream function.

The thermal dynamic equation is used to diagnose the response of the atmosphere to thermal forcing of underlying surface, which is expressed as

$$\frac{\partial\theta}{\partial t} = -V \cdot \nabla_h\theta - \omega\frac{\partial\theta}{\partial p} + \frac{\theta Q}{TC_p},$$

where the first, second, and third terms on the right-hand side represent dynamic heating from the horizontal advection of the potential temperature, dynamic heating from convection, and diabatic heating, respectively.

According to the method of Huang (2004), the EAP index is defined as

Table 1 Number of stations with different ranking of precipitation since 1962 and their percentage in total stations

Rank	Number	Percentage
1st–2nd	32	60.4
3rd–9th	17	32.1
≥ 10th	4	7.5

$$I_{EAP} = -0.25Z'_s(60°N, 125°E) + 0.50Z'_s(40°N, 125°E) - 0.25Z'_s(20°N, 125°E),$$

where $Z'_s = Z' \sin 45° / \sin\phi$ is the standardized midsummer-mean 500 hPa geopotential height anomaly at a grid point with the latitude ϕ, and $Z' = Z - \overline{Z}$ is the midsummer-mean 500 hPa geopotential height anomaly at the grid point.

3 Results

3.1 Extreme drought in Liaoning Province during midsummer 2014 and local circulation features

The spatial distribution of precipitation in Liaoning Province was non-uniform in midsummer 2014 (Fig. 1a). The maximum precipitation occurred in southeastern Liaoning Province and the minimum in the west. There was an overall gradual decrease in precipitation from east to west. The total precipitation was less than the climatological mean precipitation, with a maximum negative anomaly lower than − 190 mm (Fig. 1b). The time series of the mean total precipitation anomalies over Liaoning Province (Fig. 1c) indicated that the precipitation varied significantly on both interannual and interdecadal timescales. The total precipitation anomaly during midsummer 2014 was − 168 mm, the lowest since 1962.

During midsummer 2014, many stations in Liaoning Province experienced the lowest and the second lowest precipitation, whose percentage was as high as 60.4%. 92.5% of the stations had the 1st to 9th lowest precipitation rank (Table 1). Only seven rainfall events with a regionally average rainfall > 5 mm·day^{-1} occurred in Liaoning Province during midsummer 2014 (Table 2). This small number of rainy days and lower rainfall at most stations caused the drought in Liaoning Province in midsummer 2014.

Liaoning Province was controlled by descending air during midsummer 2014 (Fig. 2a, b). The anomalous zonal–vertical circulation (Fig. 2a) is represented by the vertical velocity and the divergent component of the zonal wind averaged over 38.6–43.6 °N. Strong anomalous downdrafts could be seen in the region between 118.6 and 126.0 °E (Liaoning Province). Strong anomalous upward motion was observed in the region between 135 and 150 °E, where existing the

Table 2 Dates of regional mean precipitation > 5 mm·day^{-1} in Liaoning Province during midsummer 2014

2014 dates	Precipitation (mm·day^{-1})
17 July	11.6
21 July	32.7
22 July	8.3
25 July	7.6
23 August	8.2
24 August	12.3
25 August	11.7

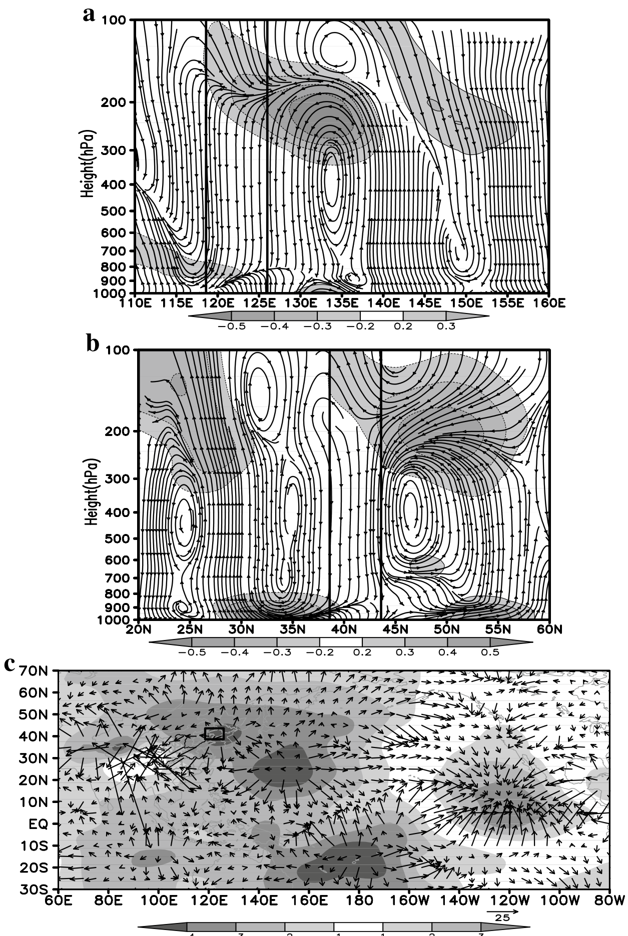

Fig. 2 **a** Anomalous zonal–vertical circulation averaged over 38.6–43.6° N, with shading indicating the zonal component of the divergent wind anomalies (m·s^{-1}). **b** Anomalous meridional–vertical circulation averaged over 118.6–126.0° E, with shading indicating the meridional component of the divergent wind anomalies (m·s^{-1}). **c** Anomalies in the water vapor flux integrated from the Earth's surface up to 300 hPa (vectors; kg·m^{-1}·s^{-1}) and the velocity potential of the water vapor flux (shading and contours; 10^6 m^2·s^{-1}) during midsummer 2014. Black rectangles in (**c**) denotes the region of Liaoning Province

maximum SSTAs in the Sea of Japan and the northwestern Pacific Ocean. The anomalous meridional–vertical circulation (Fig. 2b), with a strong anomalous branch of downward motion, was also observed over Liaoning Province in the region between 38.6 and 43.6 °N. There were two symmetrical abnormal circulations in the south and north of Liaoning Province, which strengthened the downward motion.

Water vapor diverged from Liaoning Province into the surrounding region (Fig. 2c), which did not favor the production of rainfall in Liaoning Province. A strong center of divergence of water vapor flux was located in Liaoning Province and the western Pacific, with one strong center of water vapor convergence in the eastern Pacific. This distribution of water vapor transport corresponded to the lack of rainfall in Liaoning Province. There was also a strong center of water vapor convergence in the Tibetan Plateau, but weak water vapor convergence was seen from south China to Japan.

Changes in the local anomalous circulation directly affect the anomalous precipitation. Liaoning Province was controlled by an anomalous anticyclonic circulation in the lower troposphere (Fig. 3a) and there was an anomalous anticyclone in the western Pacific to the southeast of Japan and a trough between these two regions. There was an anomalous cyclone in the mid-troposphere (Fig. 3b) over the Sea of Japan and Liaoning Province was controlled by the northeastern airflow on the western side of this anomalous cyclone. There were two anomalous anticyclones over the island of Taiwan and the western Pacific. The circulation pattern in the upper troposphere (Fig. 3c) was similar to that in the mid-troposphere, although the center of the anomalous cyclone shifted to northeast China and there were two anomalous anticyclones at low latitudes. Liaoning Province was located exactly under the area of anomalous divergence in the lower and mid-troposphere and the area of anomalous convergence in the upper troposphere, resulting in an abnormal downdraft locally.

3.2 Teleconnections at mid- and high latitudes

The local factors that facilitated the severe negative anomalous precipitation in midsummer 2014 were the divergence of water vapor and the strong descending air. The reason for this severe drought event in midsummer 2014 over Liaoning Province deserves further investigation. Figure 4 shows the circulation anomalies related to the upstream perturbations of the westerlies in midsummer 2014.

A positive–negative–positive wave train structure was observed in the East Asian–Pacific region from south to north in the lower, mid- and upper tropopause. Especially, the wave train structures in geopotential height

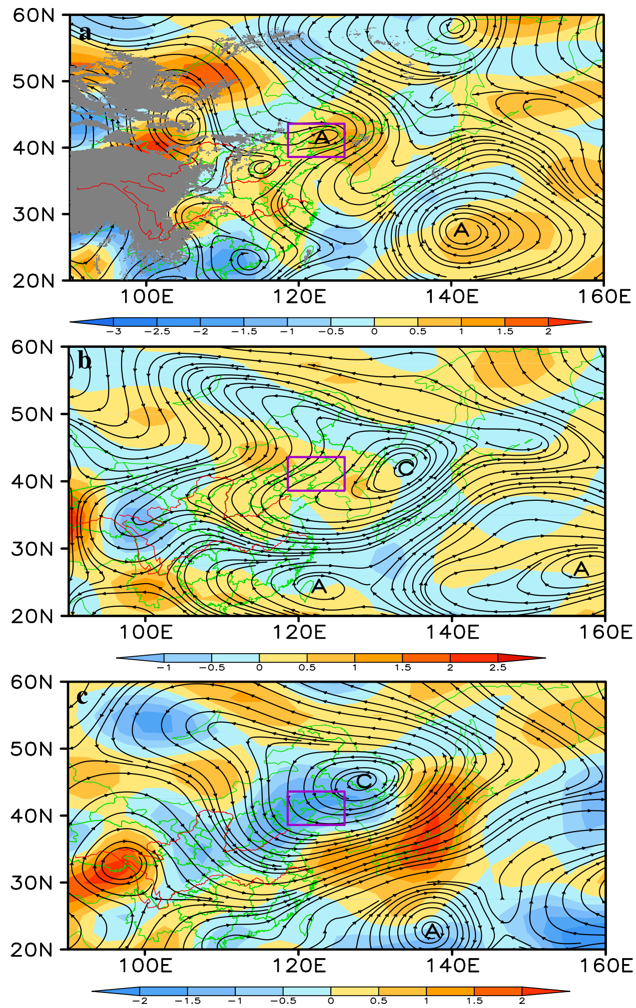

Fig. 3 Anomalous rotational wind (stream) and divergence (shading) at **a** 850, **b** 500, and **c** 200 hPa during midsummer 2014. Purple rectangles denote the region of Liaoning Province. The letters "A" and "C" represent the anomalous anticyclone and cyclone, respectively

anomalies could be seen clearly at 500 hPa (Fig. 4b) and 200 hPa (Fig. 4c). Positive geopotential height anomalies were observed from the Philippines to the western Pacific, negative geopotential height anomalies from north China to Japan and its eastern ocean, and positive geopotential height anomalies from Siberia to the Russian Far East. This distribution of geopotential height anomalies was consistent with the EAP teleconnection (Huang and Li 1987) structure and contributed to the more southward position of the WPSH and the weakened EASM, causing decreased precipitation in northeast Asia (Wang and He 2015) and increased precipitation in south China (He 2015). The structure of sea-level pressure (SLP) anomalies was different from the geopotential height anomalies at 500 and 200 hPa. Positive SLP anomalies could be seen over most of China, south Japan and its southern ocean; negative SLP anomalies were observed over most of Siberia, north Japan and its eastern ocean; and positive SLP anomalies over the Kamchatka Peninsula. There was a clear baroclinic structure over Liaoning Province.

The geopotential height anomalies at 500 and 200 hPa (Fig. 4b, c) showed a positive–negative–positive–negative–positive–negative wave train structure in mid-latitudes from southern Greenland eastward to western Europe, the Black Sea–Aral Sea, Lake Balkhash, western China and eastern China–Japan. This wave train structure led to positive–negative–positive–negative SLP anomalies from southern Greenland eastward to western Europe and the Caspian Sea, the Black Sea and most of China, and the Sikhote Mountains to southern Japan (Fig. 4a). Anticyclone–cyclone–anticyclone–cyclone anomalies were correspondingly observed at 850 hPa from northern Africa and western Europe to the northwestern Pacific (Fig. 5a). The wave train structure was consistent with the SR pattern (Lu et al. 2002; Enomoto et al. 2003). A positive–negative–positive wave train structure was seen at high latitudes (60°N–80°N, 20°W—180°E) from northern Europe to Siberia and the Russian Far East at 500 and 200 hPa (Fig. 4b, c), consistent with the EU pattern (Wallace and Gutzler 1981).

The Rossby wave energy dispersed eastward from North Atlantic played an important part in the formation and maintenance of the EAP pattern (Wang et al. 2017; Xu et al. 2017; Wang and He 2015; Shi et al. 2009). Rossby wave energy dispersed eastward along the EU pattern at high latitudes and converged in the Russian Far East, reinforcing the northern-most geopotential height anomalies center of the negative phase of EAP pattern. Meanwhile, Rossby wave energy dispersed eastward along the SR pattern at mid-latitudes and, when the energy reached East Asia, it converged with the Rossby wave energy that dispersed northward from the South China Sea and the western Pacific to east China and Japan, strengthening the geopotential height anomalies centers of the negative phase of EAP pattern located at mid- and lower latitudes. As a result, the WPSH shifted southward, contributing to the weaker EASM. The cold air was, therefore, stronger than normal, but the warm air was weaker and it was difficult to produce precipitation in Liaoning Province.

Shi et al. (2009) found that the Rossby wave energy originated from the northeastern Atlantic in the upper and middle troposphere, which propagated through Lake Balkhash and turns northeastward to northeast Asia, playing an important role in the formation and maintenance of the northern-most geopotential height anomalies center of the EAP pattern. Wang et al. (2017) and Xu et al. (2017) also revealed that the Rossby waves originated from the North Atlantic along the westerly jet stream waveguide dispersed to East Asian-Pacific region, enhancing the geopotential height anomalies center of the EAP pattern at high latitude and hence contributing to its maintenance and development. The

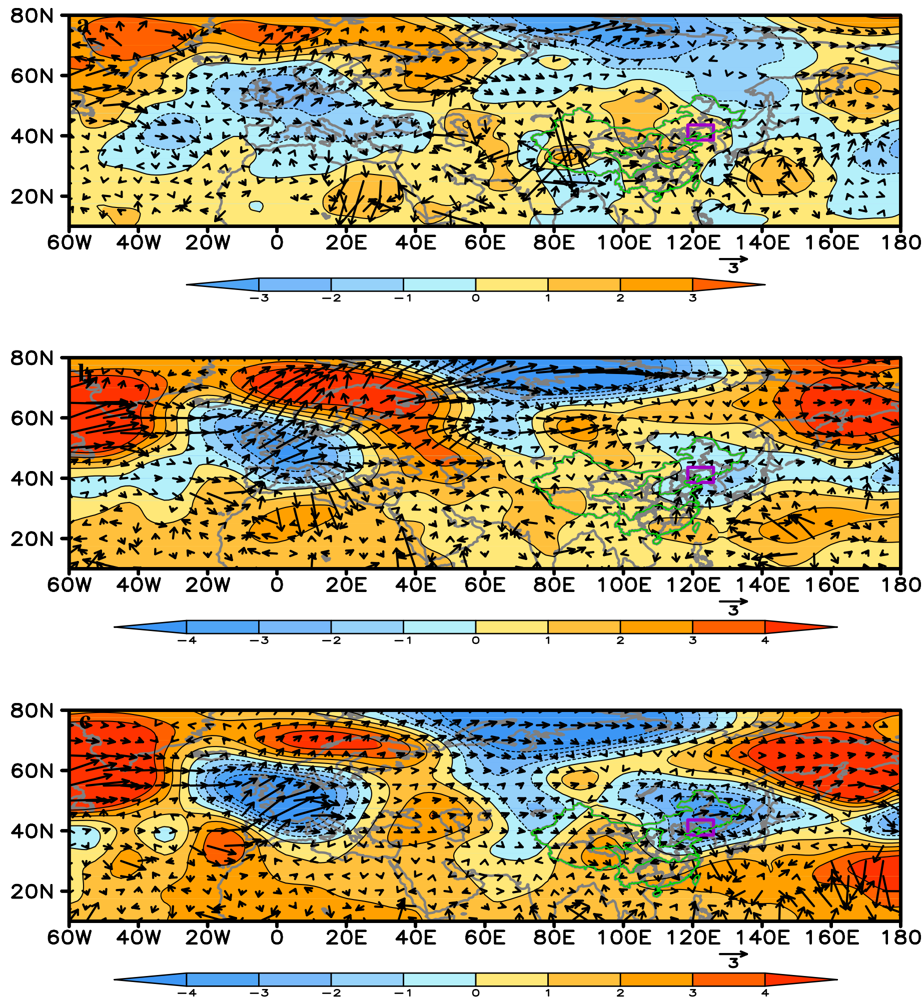

Fig. 4 **a** Sea-level pressure anomalies (shading; hPa) and wave activity flux at 850 hPa (vectors; $m^2 \cdot s^{-2}$) during midsummer 2014. **b** Geopotential height anomalies (shading; dagpm) and wave activity flux at 500 hPa (vectors; $m^2 \cdot s^{-2}$) during midsummer 2014. **c** Geopotential height anomalies (shading; dagpm) and wave activity flux at 200 hPa (vectors; $m^2 \cdot s^{-2}$) during midsummer 2014. Purple rectangles denote the region of Liaoning Province

correlation coefficient between the standardized EAP index and the midsummer precipitation anomalies time series in Liaoning Province was 0.253, which was significant at the 90% confidence level, and further demonstrated the important influence of the negative phase of EAP pattern on this extreme event.

3.3 Impacts of thermal forcing over the Pacific and Indian oceans

The SSTAs (Fig. 5a) were positive in the equatorial Pacific during midsummer 2014. In the north of the equatorial Pacific and west of 160 °W, the SSTAs presented a positive–negative–positive sandwich structure from the warm pool of the western Pacific at low latitudes to the northern Pacific at high latitudes. In particular, the positive SSTAs in the northern Pacific north of 40 °N were significant and the distribution pattern was similar to the EAP pattern of the teleconnection structure. The SSTAs were positive in most of the Indian Ocean and were relatively higher in the north and lower in the south. The responses of the atmosphere to the underlying surface thermal forcing were as follows. Positive anomalies of diabatic heating were found in the Maritime Continental (MC) region, whereas negative anomalies of diabatic heating were found in northwest Pacific (Fig. 5d). The diabatic heating was balanced by the dynamic cooling caused by the ascending motion of the MC region and the dynamic heating caused by atmospheric subsidence over the northwestern Pacific (Fig. 5c). Positive anomalies of diabatic heating were observed in the northern equatorial Indian Ocean, whereas negative anomalies were observed in the southern equatorial Indian Ocean (Fig. 5d). Diabatic heating was balanced by dynamic cooling caused by the ascending motion of the northern equatorial Indian Ocean and dynamic heating caused by atmospheric subsidence over the southern equatorial Indian Ocean (Fig. 5c).

The anomalous heating could induce circulation anomalies. The circulation anomalies caused by thermodynamic forcing can be explained by Fig. 6. There were two strong centers of divergence in the southern equatorial Indian Ocean and the northwestern Pacific in the lower troposphere and two strong centers of convergence over the Indo-China

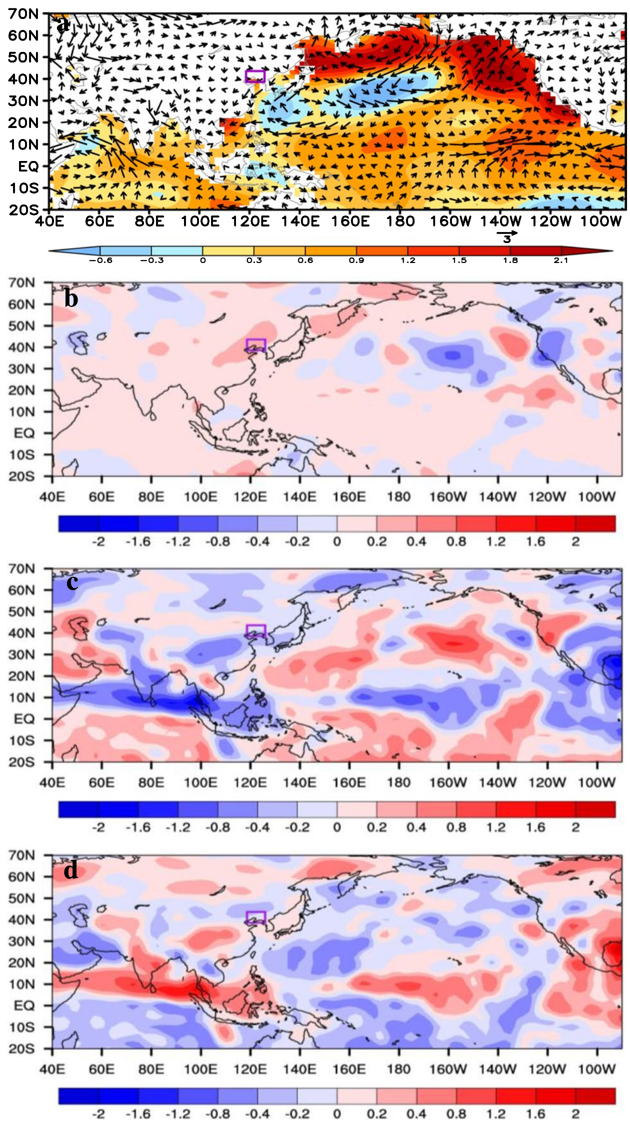

Fig. 5 **a** Sea surface temperature anomalies (shading; ℃) and wind field anomalies at 850 hPa (vectors; m·s^{-1}) during midsummer 2014. **b** Anomalies of dynamic heating (shading; K·day^{-1}) obtained by integrating the horizontal advection of potential temperature vertically from the Earth's surface up to 100 hPa during midsummer 2014. **c** Anomalies of dynamic heating (shading; K·day^{-1}) obtained by integrating the convection of potential temperature vertically from the Earth's surface up to 100 hPa during midsummer 2014. **d** Anomalies of vertically integrated diabatic heating (shading; K·day^{-1}) during midsummer 2014. Purple rectangles denote the region of Liaoning Province

Peninsula and the MC region (Fig. 6a). Two centers of divergence in the Japanese archipelago and east of the Indonesian islands and two strong centers of convergence over the Bay of Bengal and the western Pacific were seen in the upper troposphere (Fig. 6c). The anomalous winds caused by the SSTAs converged over the Indo–China Peninsula and the MC region from the southern equatorial Indian Ocean and the western Pacific in the lower troposphere (Fig. 6a). The anomalous winds converged into the Bay of Bengal and the western Pacific from the Japanese archipelago and east of the Indonesian islands in the upper troposphere (Fig. 6c). Affected by this, the anomalous winds diverged in the lower troposphere (Fig. 6a) and converged in the upper troposphere (Fig. 6c) over Liaoning Province, resulting in an anomalous downdraft (Figs. 2b and 6a). The SSTAs in the Indian Ocean were positive, indicating that the difference in thermal energy between the land and sea was weakened. The EASM was, therefore, weak, resulting in an insufficient flow of warm and wet air toward Liaoning Province (Figs. 2c and 5a).

4 Summary and conclusions

We studied the extreme drought event in Liaoning Province during midsummer 2014 using the NCEP/NCAR monthly reanalysis product, the NOAA extended reconstructed SSTs, and daily rainfall data from 53 observational stations. Our conclusions are as follows.

Liaoning Province experienced the most severe drought since 1962 in midsummer 2014. This event was marked by an unusual lack of rainfall and a low number of rainy days. The anomalous circulation over Liaoning Province was baroclinic during the drought event and a center of divergence was observed in the lower troposphere. Water vapor diverged away from Liaoning Province. There were two important factors responsible for the formation of the circulation anomalies over Liaoning Province.

The effect of large-scale circulations on this extreme drought event was schematically illustrated in Fig. 7. One factor was the teleconnections in mid- and high latitudes related to the EAP, EU and SR patterns. The position of WPSH was affected by the negative phase of EAP pattern and was further south than normal. The EASM was, therefore, weakened, contributing to the southward location of the rain belt. The dispersion of energy from Rossby waves was one of the main causes of the formation and maintenance of the EAP pattern. The Rossby wave energy dispersed eastward along the EU pattern at high latitudes, reinforcing the northern-most geopotential height anomalies center of the negative phase of EAP pattern. The energy dispersed eastward along the SR pattern at mid-latitudes, strengthening the geopotential height anomalies centers of the negative phase of EAP pattern in mid- and lower latitudes. The negative phase of EAP pattern was ultimately maintained. As a result, the WPSH shifted southward, contributing to the weaker EASM. It was, therefore, difficult to produce precipitation in Liaoning Province.

The other factor responsible for the formation of the circulation anomalies over Liaoning Province was anomalous thermal forcing in the northwestern Pacific, the MC

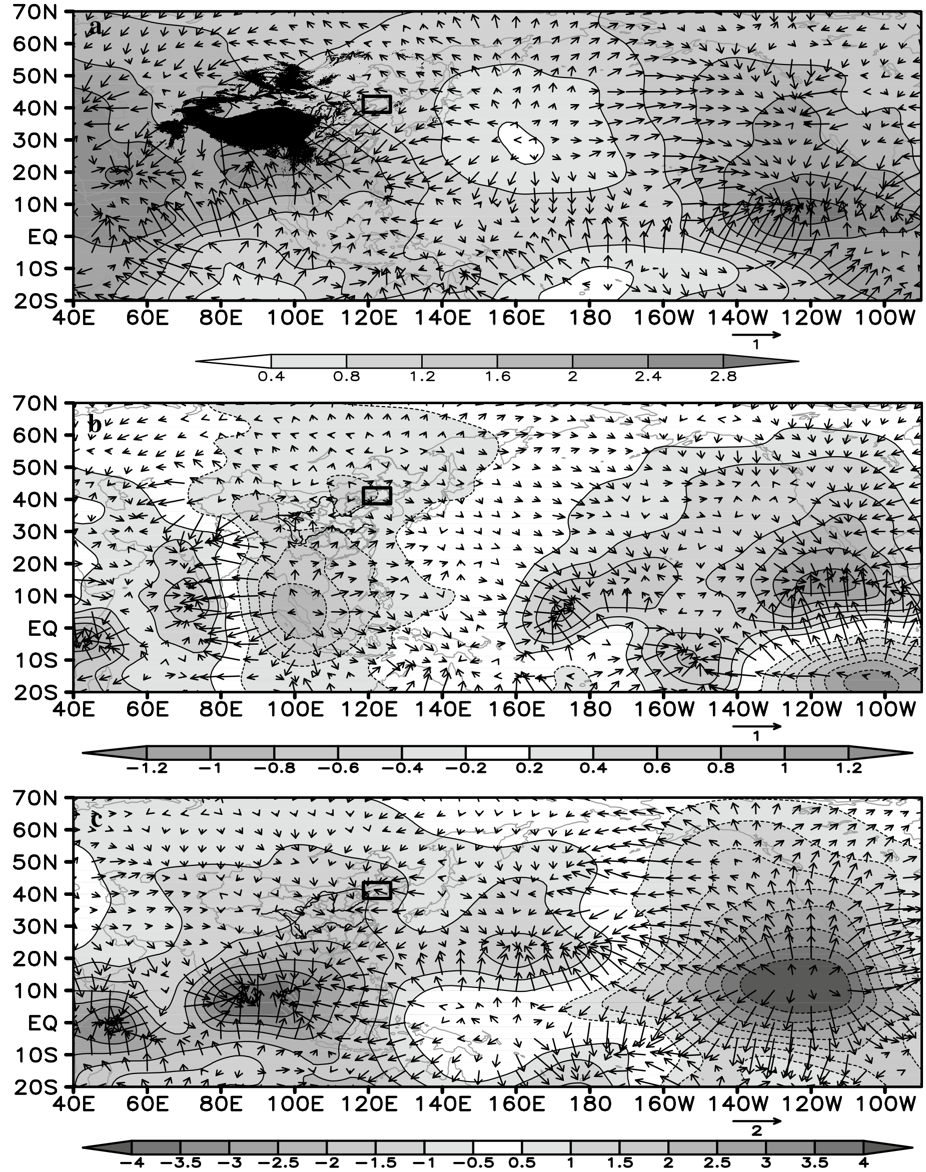

Fig. 6 Anomalous velocity potential (shading and contours; 10^6 $m^2 \cdot s^{-1}$) and related divergent component of winds (vectors; $m \cdot s^{-1}$) at **a** 850, **b** 500, and **c** 200 hPa during midsummer 2014. Black rectangles denote the region of Liaoning Province

region, and the Indian Ocean. The SSTAs were positive in the equatorial Pacific and most of the Indian Ocean during midsummer 2014. The SSTAs presented a positive–negative–positive sandwich structure from the warm pool of the western Pacific at low latitudes to high latitudes to the north of the equatorial Pacific and to the west of 160° W. The anomalous winds affected by thermal forcing converged into the Indo-China Peninsula and the MC region from the southern equatorial Indian Ocean and the western Pacific in the lower troposphere and converged into the Bay of Bengal and the western Pacific from the Japanese archipelago and east of the Indonesian islands in the upper troposphere, resulting in an anomalous downdraft over Liaoning Province. The SSTAs in the Indian Ocean were positive, resulting in a weakened difference in thermal energy between the land and sea. The EASM was, therefore, weak and the lessened warm and wet air flow delivered to Liaoning Province led to the midsummer drought.

Acknowledgements We are grateful to the NOAA and the Meteorological Information Center of Liaoning Province for providing the datasets.

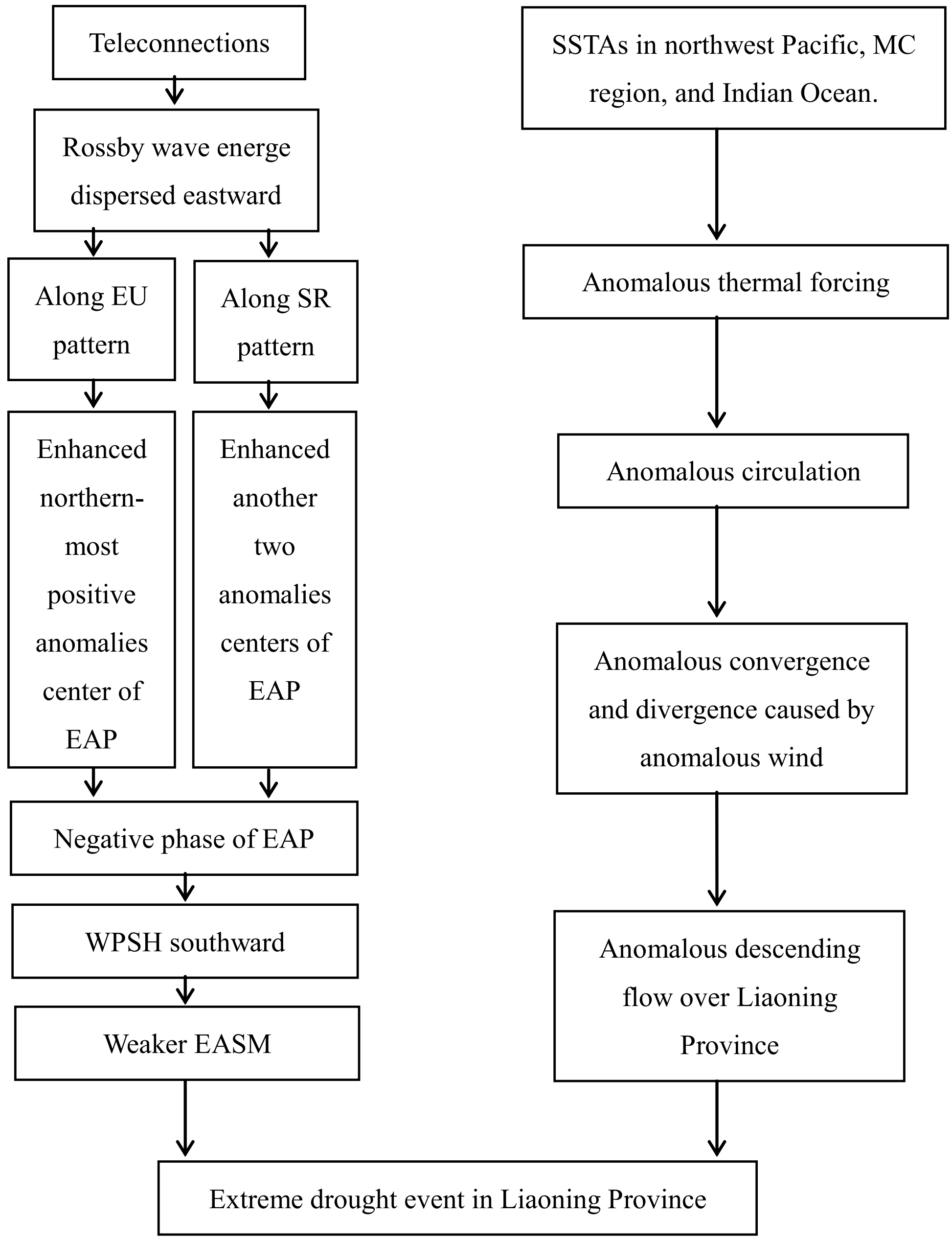

Fig. 7 Sketch map of the effect of large-scale circulations on extreme drought event in Liaoning Province in midsummer 2014

Author contributions All the authors contributed to the study conception and design. Material preparation, data collection and analysis were performed by [Wei HUANG], [Liqiang CHEN], [Fenghua Sun], and [Zenghua YU]. The first draft of the manuscript was written by [Min JIAO], and all the authors commented on previous versions of the manuscript. All the authors read and approved the final manuscript.

Funding This study was supported by the National Key Research and Development Program Subject (2018YFC1505601) and Joint Opening Fund of Key Project for Institute of Atmospheric Environment, China Meteorological Administration, Shenyang and Key Opening Laboratory for Northeast China Cold Vortex Research (2020SYIAEZD5).

Availability of data and material The NCEP/NCAR monthly reanalysis product and the extended reconstructed SST dataset are provided by NOAA, which are available free at their website (www.esrl.noaa.gov/psd/). The daily rainfall data collected at 53 observational stations is provided by the Meteorological Information Center of Liaoning Province.

Code availability The figures in this paper were prepared with GrADS and NCL software.

Declarations

Conflict of interest The authors declare that they have no conflicts of interest.

References

Barriopedro D, Gouveia CM, Trigo RM, Wang L (2012) The 2009/10 drought in China: possible causes and impacts on vegetation. J Hydrometeorology 13(4):1251–1267. https://doi.org/10.1175/JHM-D-11-074.1

Enomoto T, Hoskins BJ, Matsuda Y (2003) The formation mechanism of the Bonin high in August. Quarter J Royal Meteorol Soc 129(587):157–178. https://doi.org/10.1256/qj.01.211

Gao H, Gao J (2014) Increased influences of the SST along the Kuroshio in previous winter on the summer precipitation in northeastern China. Acta Oceanol Sin 36(7):27–33. https://doi.org/10.3969/j.issn.0253-4193.2014.07.004

Gao J, Gao H (2015) Relationship between summer precipitation over northeastern China and sea surface temperature in the southeastern Pacific and the possible underlying mechanisms. Chin J Atmos Sci 39(5):967–977. https://doi.org/10.3878/j.issn.1006-9895.1503.14246

Guan ZY, Yamagata T (2003) The unusual summer of 1994 in: IOD teleconnections. Geophys Res Lett 30(10):1544–1547. https://doi.org/10.1029/2002GL016831

He SP (2015) Potential connection between the Australian summer monsoon circulation and summer precipitation over central China. Atmos Ocean Science Lett 8(3):120–126. https://doi.org/10.3878/AOSL20140091

Huang G (2004) An index measuring the interannual variation of the East Asian summer monsoon—the EAP index. Adv Atmos Sci 21(1):41–52. https://doi.org/10.1007/BF02915679

Huang RH, Li WJ (1987) Influence of the heat source anomaly over the tropical western Pacific on the subtropical high over East Asia. In: Proceedings of international conference on the general circulation of East Asia. Chengdu, China, pp 40–51

Huang RH, Huangfu JL, Liu Y, Du ZC, Chen GS, Chen W, Lu RY (2016) Development from the theory of energy dispersion of Rossby waves to studies on the dynamics of quasi-stationary planetary waves. Chin J Atmos Sci 40(1):3–21. https://doi.org/10.3878/j.issn.1006-9895.1503.14298

Jiao M, Li J, Wang Y, Wang Y, Huang Y (2018) Large-scale circulation characteristics of anomalous less rainfall in Liaoning Province in midsummer of 2014. J Arid Meteorol 36(5):751–757. https://doi.org/10.11755/j.issn.1006-7639(2018)-05-0751

Jiao M, Li J, Chen PS, Wang Y, Liu DM (2019) Analysis of circulation characteristics and cause of anomalous high temperature and drought in summer of 2018 over Liaoning. Trans Atmos Sci 42(4):571–580. https://doi.org/10.13878/j.cnki.dqkxxb.20190326001

Kalnay E, Kanamitsu M, Kistler R et al (1996) The NCEP/NCAR 40-year reanalysis project. Bull Amer Meteor Soc 77(3):437–471. https://doi.org/10.1175/1520-0477(1996)077%3c0437:TNYRP%3e2.0.CO;2

Ke D, Guan ZY (2014) Variations in regional mean daily precipitation extremes and related circulation anomalies over central china during boreal summer. J Meteor Res 28(4):524–539. https://doi.org/10.1007/s13351-014-3246-9

Kim DW, Byun HR, Choi KS, Oh SB (2011) A spatiotemporal analysis of historical droughts in Korea. J Appl Meteorol Clim 50(9):1895–1912. https://doi.org/10.1175/2011JAMC2664.1

Kurihara K, Tsuyuki T (1987) Development of the barotropic high around Japan summer weather and the subtropical high in the western North Pacific. J Meteor Soc Japan 65(2):237–246. https://doi.org/10.2151/jmsj1965.65.2_237

Li J, Li F, Hu CL, Lin R (2014) Large-scale circulation impact factors of midsummer precipitation in Liaoning Province and causes analysis of anomalous rainfall in 2010. Plateau Meteorol 33(4):1076–1085. https://doi.org/10.7522/j.issn.1000-0534.2013.00006

Li MG, Guan ZY, Mei SL (2016) Interannual and interdecadal variations of summer rainfall duration over the middle and lower reaches of the Yangtze River in association with anomalous circulation and Rossby wave activities. Chin J Atmos Sci 40(6):1199–1214. https://doi.org/10.3878/j.issn.1006-9895.1511.15257

Lu RY, Oh JH, Kim BJ (2002) A teleconnection pattern in upper-level meridional wind over the North African and Eurasian continent in summer. Tellus 54:44–55. https://doi.org/10.1034/j.1600-0870.2002.00248.x

Ma F, Luo LF, Ye AZ, Duan QY (2019) Drought characteristics and propagation in the semiarid Heihe River Basin in Northwestern China. J Hydrometeorol 20(1):59–77. https://doi.org/10.1175/JHM-D-18-0129.1

Nitta T (1987) Convective activities in the tropical western Pacific and their impact on the Northern Hemisphere summer circulation. J Meteor Soc Japan 65(3):373–390. https://doi.org/10.2151/jmsj1965.65.3_373

Saji NH, Goswami BN, Vinayachandran PN, Yamagata T (1999) A dipole mode in the tropical Indian Ocean. Nature 401(6751):360–363. https://doi.org/10.1038/43854

Schubert SD, Wang HL, Koster RD, Suarez MJ (2014) Northern Eurasian heat waves and droughts. J Chimate 27(9):3169–3207. https://doi.org/10.1175/JCLI-D-13-00360.1

Shi N, Bueh ZL, Ji LR, Wang PX (2009) Impacts of mid-and high-latitude Rossby wave activities on the medium-range evolution of /Pacific events during the mid-and late summer(in Chinese). Chin J Atmos Sci 33(5):1087–1100. https://doi.org/10.1016/S1003-6326(09)60084-4

Smith TM, Richard WR, Thomas CP, Jay L (2008) Improvements to NOAA's historical merged land–ocean surface temperature analysis (1880–2006). J Chimate 21(10):2283–2296. https://doi.org/10.1175/2007JCLI2100.1

Sun JC, Guan ZY, Li MG, Yu YX (2019) Anomalous circulation patterns in association with two types of regional daily precipitation extremes over South China from July to October. Acta Meteor Sin 77(1):43–57. https://doi.org/10.11676/qxxb2018.044

Takaya K, Nakamura H (1997) A formulation of a wave-activity flux for stationary Rossby waves on a zonally varying basic flow. Geophys Res Lett 24(23):2985–2988. https://doi.org/10.1029/97GL03094

Takaya K, Nakamura H (2001) A formulation of a phase-Independent wave-activity flux for stationary and migratory quasigeostrophic eddies on a zonally varying basic flow. J Atmos Sci 58(6):608–627. https://doi.org/10.1175/1520-0469(2001)058%3c0608:AFOAPI%3e2.0.CO;2

Wallace JM, Gutzler DS (1981) Teleconnections in the geopotential height field during the Northern Hemisphere winter. Mon Weather Rev 109:784–812. https://doi.org/10.1175/1520-0493(1981)109%3c0784:TITGHF%3e2.0.CO;2

Wang HJ, He SP (2015) The North China/Northeastern Asia severe summer drought in 2014. J Climate 28(17):6667–6681. https://doi.org/10.1175/JCLI-D-15-0202.1

Wang XF, He JH, Lian Y (2013) Effect of the previous anomalous heat content in the western Pacific warm pool on the summer rainfall over Northeast China. Acta Meteor Sin 71(2):305–317. https://doi.org/10.11676/qxxb2013.024

Wang Q, Li SL, Fu JJ (2016) The impacts of SSTA in Kuroshio and its extension on precipitation in Northeast China under the background of the different El Niño cases. J Trop Meteorol 32(1):73–84. https://doi.org/10.16032/j.issn.1004-4965.2016.01.008

Wang W, Xu JP, Cai XJ, Sun C (2017) Analysis of atmospheric circulation characteristics and mechanism of heat wave and drought in summer of 2013 over the middle and lower reaches of Yangtze

River Basin. Plateau Meteorol 36(6):1595–1607. https://doi.org/10.7522/j.issn.1000-0534.2016.00129

Wei J, Zhang QY, Tao SY (2004) Physical causes of the 1999 and 2000 summer severe drought in North China. Chin J Atmos Sci 28(1):125–137. https://doi.org/10.1091/mbc.7.4.565

Xu JP, Wang W, Cai XJ, Xu ZL, Xu JX (2017) A comparison of the Rossby wave activities and circulation features of the drought in winter-spring of 2011 and in summer of 2013 over mid-lower reaches of the Yangeze River basin. J Trop Meteorol 33(6):992–999b. https://doi.org/10.16032/j.issn.1004-4965.2017.06.020

Yang WY, Wang QQ (2006) Analyses on circulation characteristics of precipitation anomalies in flood season of Liaoning. Plateau Meteorology 25(5):969–974. https://doi.org/10.3321/j.issn:1000-0534.2006.05.027

Ye DC, Guan ZY, Sun SY, Li X, Xia Y (2019) The relationship between heavy precipitation in the middle and lower reaches of Yangtze River and baroclinic wave packets in the upper troposphere during the Meiyu period of 2016. Acta Meteor Sin 77(1):73–83. https://doi.org/10.11676/qxxb2018.038

Zhang LX, Zhou TJ (2015) Drought over: a review. J Climate 28(8):3375–3399. https://doi.org/10.1175/JCLI-D-14-00259.1

Zhang WJ, Jin FF, Zhao JX, Qi L, Ren HL (2013) The possible influence of a nonconventional El Niño on the severe autumn drought of 2009 in Southwest China. J Climate 26(21):8392–8405. https://doi.org/10.1175/JCLI-D-12-00851.1

Zhang LX, Wu PL, Zhou TJ, Xiao C (2015) ENSO transition from La Niña to El Niño drives prolonged spring-summer drought over North China. J Climate 31(9):3509–3523. https://doi.org/10.1175/JCLI-D-17-0440.1